

## High fat diet delays plasmin generation in a thrombomodulin-dependent manner in mice

Tracking no: BLD-2019-004267R1

Adam Miszta (University of North Carolina at Chapel Hill, United States) Anna Kopec (University of North Carolina at Chapel Hill, United States) Asmita Pant (Michigan State University, ) Lori Holle (University of North Carolina, United States) James Byrnes (University of California, San Francisco, United States) Daniel Lawrence (University of Michigan Medical School, United States) Kirk Hansen (UC Denver, United States) Matthew Flick (University of North Carolina, Chapel Hill, United States) James Luyendyk (Michigan State University, United States) Bas de Laat (Synapse BV, Netherlands) Alisa Wolberg (University of North Carolina at Chapel Hill, United States)

### Abstract:

Obesity is a prevalent prothrombotic risk factor marked by enhanced fibrin formation and suppressed fibrinolysis. Fibrin both promotes thrombotic events and drives obesity pathophysiology, but a lack of essential analytical tools has left fibrinolytic mechanisms affected by obesity poorly defined. Using a plasmin-specific fluorogenic substrate, we developed a plasmin generation (PG) assay that is sensitive to tissue plasminogen activator,  $\alpha_2$ -antiplasmin, active plasminogen activator inhibitor (PAI-1), and fibrin formation, but not fibrin crosslinking in mouse plasma. Compared to plasma from mice fed a control diet (CD), plasmas from mice fed a high fat diet (HFD) showed delayed PG and reduced PG velocity. Concurrent to impaired PG, HFD also enhanced thrombin generation (TG). The collective impact of abnormal TG and PG in HFD-fed mice produced normal fibrin formation kinetics but delayed fibrinolysis. Functional and proteomic analyses determined that delayed PG in HFD-fed mice was not due to altered levels of plasminogen,  $\alpha_2$ -antiplasmin, or fibrinogen. Changes in PG were also not explained by elevated PAI-1, since active PAI-1 concentrations required to inhibit the PG assay were 100-fold higher than circulating concentrations in mice. HFD-fed mice had increased circulating thrombomodulin, and inhibiting thrombomodulin or thrombin-activated fibrinolysis inhibitor (TAFI) normalized PG, revealing a thrombomodulin- and TAFI-dependent antifibrinolytic mechanism. Integrating kinetic parameters to calculate the metric of TG/PG ratio revealed a quantifiable net shift toward a prothrombotic phenotype in HFD-fed mice. Integrating TG and PG measurements may define a prothrombotic risk factor in diet-induced obesity.

**Conflict of interest:** COI declared - see note

**COI notes:** AM and BdL are employed by Synapse Research Institute, a member of the STAGO Diagnostic group that produces calibrated automated thrombography for thrombin generation measurements in plasma. None of the other authors have relevant potential conflict of interest.

**Preprint server:** No;

**Author contributions and disclosures:** AM, BdL, and ASW developed the hypothesis; AM, AKK, AP, KCH, LAH, and JRB performed experiments and/or collected data; VAP, FJC, and DAL provided essential reagents; AM, KCH, MJF, JPL, and ASW analyzed data; AM, JPL, and ASW interpreted data; AM, MJF, JPL, and ASW wrote the manuscript, which was revised and approved by all authors.

**Non-author contributions and disclosures:** No;

**Agreement to Share Publication-Related Data and Data Sharing Statement:** Publication-related data available by download or upon request to the corresponding author.

**Clinical trial registration information (if any):**

# High fat diet delays plasmin generation in a thrombomodulin-dependent manner in mice

## Running title: High fat diet delays plasmin generation

Adam Miszta<sup>1,2,3</sup>, Anna K. Kopec<sup>4</sup>, Asmita Pant<sup>4</sup>, Lori A. Holle<sup>1</sup>, James R. Byrnes<sup>1</sup>, Daniel A. Lawrence<sup>5</sup>, Kirk C. Hansen<sup>6</sup>, Matthew J. Flick<sup>1</sup>, James P. Luyendyk<sup>4</sup>, Bas de Laat<sup>2,3</sup>, Alisa S. Wolberg<sup>1</sup>

<sup>1</sup> Department of Pathology and Laboratory Medicine and UNC Blood Research Center, University of North Carolina at Chapel Hill, Chapel Hill, North Carolina, USA

<sup>2</sup> Synapse Research Institute, Maastricht, the Netherlands

<sup>3</sup> Department of Biochemistry, CARIM, Maastricht University Medical Center, Maastricht, The Netherlands

<sup>4</sup> Department of Pathobiology and Diagnostic Investigation, Institute for Integrative Toxicology, Michigan State University, East Lansing, Michigan, USA

<sup>5</sup> Department of Internal Medicine, University of Michigan Medical School, Ann Arbor, Michigan, USA

<sup>6</sup> Department of Biochemistry and Molecular Genetics, University of Colorado, Denver, Colorado, USA

Address correspondence to:

Alisa S. Wolberg, Ph.D.

Department of Pathology and Laboratory Medicine

University of North Carolina at Chapel Hill

8018A Mary Ellen Jones Building, CB #7035

Chapel Hill, NC 27599-7035

Phone: (919) 962-8943; Fax: (919) 843-4896

Email: [alisa\\_wolberg@med.unc.edu](mailto:alisa_wolberg@med.unc.edu)

## KEY POINTS

- A novel assay reveals delayed plasmin generation in plasma from mice fed a high-fat diet.
- Proteomic and functional analyses suggest delayed plasmin generation results from a thrombomodulin- and TAFI-dependent mechanism.

## ABSTRACT

Obesity is a prevalent prothrombotic risk factor marked by enhanced fibrin formation and suppressed fibrinolysis. Fibrin both promotes thrombotic events and drives obesity pathophysiology, but a lack of essential analytical tools has left fibrinolytic mechanisms affected by obesity poorly defined. Using a plasmin-specific fluorogenic substrate, we developed a plasmin generation (PG) assay that is sensitive to tissue plasminogen activator,  $\alpha_2$ -antiplasmin, active plasminogen activator inhibitor (PAI-1), and fibrin formation, but not fibrin crosslinking in mouse plasma. Compared to plasma from mice fed a control diet (CD), plasmas from mice fed a high fat diet (HFD) showed delayed PG and reduced PG velocity. Concurrent to impaired PG, HFD also enhanced thrombin generation (TG). The collective impact of abnormal TG and PG in HFD-fed mice produced normal fibrin formation kinetics but delayed fibrinolysis. Functional and proteomic analyses determined that delayed PG in HFD-fed mice was not due to altered levels of plasminogen,  $\alpha_2$ -antiplasmin, or fibrinogen. Changes in PG were also not explained by elevated PAI-1, since active PAI-1 concentrations required to inhibit the PG assay were 100-fold higher than circulating concentrations in mice. HFD-fed mice had increased circulating thrombomodulin, and inhibiting thrombomodulin or thrombin-activated fibrinolysis inhibitor (TAFI) normalized PG, revealing a thrombomodulin- and TAFI-dependent antifibrinolytic mechanism. Integrating kinetic parameters to calculate the metric of TG/PG ratio revealed a quantifiable net shift toward a prothrombotic phenotype in HFD-fed mice. Integrating TG and PG measurements may define a prothrombotic risk factor in diet-induced obesity.

## KEYWORDS

Plasmin, thrombin, obesity, thrombomodulin, thrombosis, fibrinogen, fibrin, PAI-1, mice, diet

## INTRODUCTION

Obesity and its affiliated sequelae such as cardiovascular disease, type II diabetes, nonalcoholic fatty liver disease, and cancer are leading causes of morbidity and mortality.<sup>1-5</sup> Obesity is a risk factor for thrombotic disorders including stroke, myocardial infarction, and venous thromboembolism, and increases thrombotic risk associated with acquired risk factors.<sup>1-5</sup> However, mechanisms controlling the prothrombotic ramifications of obesity remain poorly understood.

Obesity is an inflammatory condition associated with altered expression of coagulation factors by the diseased liver and inflamed endothelium. For example, plasma levels of procoagulant factors VII, VIII, von Willebrand factor, and fibrinogen are increased in obese humans and in mice with diet-induced obesity.<sup>6-11</sup> These abnormalities enhance thrombin generation (TG), which is demonstrable using established methods that quantify *in vivo* activation of coagulation (e.g., thrombin-antithrombin complexes [TAT]) or procoagulant potential (e.g., TG assay).<sup>12</sup> Indeed, TG is increased in obese patients and associates with visceral adiposity.<sup>13, 14</sup> Overall, strong evidence suggests that a greater propensity to generate thrombin and produce fibrin contributes to the prothrombotic state in obesity.

Fibrin formation is counter-balanced by the fibrinolytic system. Fibrin formation stimulates activation of plasminogen to the enzyme plasmin that mediates fibrin degradation. Multiple studies have detected abnormal expression of proteins that regulate plasmin generation (PG) and plasmin activity in obese humans and mice, including tissue plasminogen activator [tPA], plasminogen activator inhibitor-1 [PAI-1],  $\alpha_2$ -antiplasmin, and thrombin-activated fibrinolysis inhibitor [TAFI].<sup>8, 10, 11, 15-19</sup> Fibrinolysis end products (e.g.,  $\alpha_2$ -antiplasmin-plasmin complexes [PAP], D-dimer) are also elevated in obese humans and mice.<sup>17, 20</sup> However, compared to procoagulant function, fewer methods are available to assess fibrinolytic potential. Thromboelastography, turbidimetry, and the euglobulin clot lysis time detect fibrin formation and lysis, but do not provide quantitative information on the kinetics of PG. Previous methods to measure PG kinetics in plasma incorporated the use of fluorogenic substrates<sup>21-23</sup>; however, these have not been applied to obesity. Moreover, these methods did not correct for  $\alpha_2$ -macroglobulin-trapped plasmin ( $\alpha_2$ M-Pm) or inner filter effects (adsorption of light by non-fluorescent proteins). Thus, whereas considerable insight is available into mechanisms altering thrombin activity and initial fibrin formation in obesity, less is known about the quantitative dynamics of plasmin. This knowledge gap is a barrier to a complete understanding of the fibrinolytic derangement and prothrombotic state that is a highly prevalent characteristic of obesity.

In this study, we describe the development and characterization of a new kinetic assay that reveals PG potential in mouse plasma. Application of this assay to an experimental setting of high fat diet (HFD)-induced obesity revealed a thrombomodulin- and TAFI-dependent mechanism that delays PG in plasma from HFD-fed mice. Our study reveals a complementary analytic strategy and identifies a new metric, the TG/PG ratio, to characterize the hemostatic imbalance associated with prothrombotic disease.

## **MATERIALS AND METHODS**

Materials and methods can be found in the accompanying Supplement.

## RESULTS

**PG assay development.** To study potential effects of obesity on plasmin generation we first developed a new PG assay using a calibrated, automated method based on established principles used to measure TG (Figure 1A). Briefly, PG is triggered by addition of human tissue factor (TF) and recombinant human tPA (rtPA) to recalcified mouse plasma. Subsequent cleavage of a fluorogenic substrate by plasmin generates a fluorescent signal which is calibrated against human  $\alpha_2$ M-Pm complexes to correct for the inner filter effect, and then transformed into a PG curve. Similar to TG, PG is characterized by an initiation phase that precedes plasmin detection. The initiation phase is followed by a burst of PG and subsequent inhibition of active plasmin. Comparison of PG curves obtained in the presence of fluorogenic substrate with curves obtained from reactions in which wells were subsampled into fluorogenic substrate showed that the substrate, itself, does not alter PG kinetics (Supplemental Figure 1A). Turbidity measurements confirmed this finding, showing that the plasmin fluorogenic substrate did not change fibrin formation kinetics or clot stability (Supplemental Figure 1B). Substrate specificity was confirmed as PG was not detected in plasma from *Plg<sup>-/-</sup>* mice (Figure 1B) and was reduced by addition of mouse  $\alpha_2$ -antiplasmin in reactions triggered by either high or low rtPA (Figure 1C-D, respectively).

Since mouse plasma must be diluted for TG assays<sup>24</sup>, we tested the impact of plasma dilution on PG (Figure 1E). Dilution did not affect the lagtime but significantly shortened the time to peak (TtPeak), although the overall change was small (Supplemental Figure 2A-B). Dilution slightly but non-significantly increased velocity and decreased the peak (Supplemental Figure 2C-D). The total amount of plasmin generated (EPP) decreased with plasma dilution (Supplemental Figure 2E). Table 1 shows intra-assay, inter-assay, and inter-mouse variation for 1:3 and 1:6 dilutions of plasma. Intra-assay variation for each parameter was below 10%. Except for lagtime and velocity, inter-assay variation was below 15%. Inter-mouse variation was comparable to that of TG parameters in human plasma.<sup>25</sup>

**Exogenous rtPA increases PG.** PG was not observed in the absence of rtPA, indicating basal levels of circulating tPA or uPA (~1-5 ng/mL)<sup>26, 27</sup> are not sufficient to trigger measurable PG (data not shown). Addition of exogenous rtPA (0.31-10  $\mu$ g/mL) shortened the lagtime and TtPeak and increased the velocity, peak, and EPP in a concentration-dependent manner (Figure 1F-G, Supplemental Figure 2F-J). Although velocity, peak, and EPP were higher in 1:3 than 1:6 diluted plasma, qualitative effects were similar. We used 0.31 and 1.25  $\mu$ g/mL rtPA for subsequent experiments.

**PG requires fibrin formation, but not fibrin crosslinking.** During coagulation, thrombin cleaves fibrinopeptides from fibrinogen, producing fibrin monomers. Monomers then assemble into fibrin fibers, which function as a cofactor for plasminogen activation.<sup>28, 29</sup> To characterize relationships between TG, fibrin formation, and PG, we tested plasmas from wild-type mice and mice with deficiencies or abnormalities in fibrinogen concentration or fibrin assembly. As expected, compared to *Fga*<sup>+/+</sup> mice, partial deficiency in fibrinogen (*Fga*<sup>+/-</sup>) did not alter TG (Figure 1H), but significantly decreased fibrin formation (Figure 1I) and reduced the PG velocity, peak, and EPP (Figure 1J, Supplemental Figure 3A-E). *Fga*<sup>-/-</sup> mice showed normal plasma TG but did not form fibrin or generate plasmin (Figure 1H-J, Supplemental Figure 3A-E). To determine whether effects of fibrinogen deficiency on PG were due to loss of fibrinogen or decreased fibrin formation, we tested plasmas from mice expressing normal levels of a mutant fibrinogen that cannot polymerize (*Fgn*<sup>AEK</sup>).<sup>30</sup> TG did not differ in plasma from *Fgn*<sup>WT/WT</sup> and *Fgn*<sup>AEK/AEK</sup> mice (Figure 1K); however, turbidity experiments showed decreased and no fibrin formation in plasma from *Fgn*<sup>WT/AEK</sup> and *Fgn*<sup>AEK/AEK</sup> mice, respectively (Figure 1L). Compared to *Fgn*<sup>WT/WT</sup> mice, plasma from *Fgn*<sup>WT/AEK</sup> mice had a reduced peak and EPP, and plasma from *Fgn*<sup>AEK/AEK</sup> mice did not support PG (Figure 1M, Supplemental Figure 3F-J). There was no difference in TG, fibrin formation, or PG in plasmas from *F13a1*<sup>+/+</sup>, *F13a1*<sup>+/-</sup>, and *F13a1*<sup>-/-</sup> mice (Figure 1N-P, Supplemental Figure 3K-O) or in wild-type plasma treated with the factor XIIIa inhibitor, T101 (Supplemental Figure 3U). These findings indicate the PG assay is strongly dependent on fibrin polymerization, but not fibrin crosslinking.

We also varied TF (0.05-6 pM) to characterize the role of TG in fibrin formation and PG. Increasing TF shortened the lagtime for TG, fibrin formation, and PG, demonstrating a positive correlation between the onset of these events (Figure 1Q-S, Supplemental Figure 3P). As anticipated, increasing TF also shortened the TG TtPeak and increased the velocity, peak, and ETP (Figure 1Q, Supplemental Figure 3Q-T). In clot formation assays, increasing TF decreased the maximum clot turbidity (Figure 1R), consistent with prior observations that higher thrombin produces clots with thinner fibrin fibers.<sup>31</sup> Increasing TF did not alter the PG TtPeak, velocity, peak, or EPP (Figure 1S, Supplemental Figure 3Q-T), likely due to the relatively high rtPA concentration.<sup>32</sup> Findings were similar in 1:6- and 1:3- diluted plasma (Figure 1Q-S and data not shown). Collectively, these data suggest fibrin formed from even low thrombin is sufficient to enable PG.

**HFD-fed mice demonstrate hypercoagulable and hypofibrinolytic states.** To assess the effect of obesity on PG we then studied mice fed a control diet (CD) or high fat diet (HFD) for 12 weeks. As anticipated,<sup>9</sup> mice fed a HFD for 12 weeks gained more weight than did mice fed a CD (Figure 2A). HFD-fed mice developed liver

injury indicated by significantly elevated serum alanine aminotransferase (ALT) activity (Figure 2B), which correlated with body weight ( $R=0.855$ ,  $P<0.003$ ). Histopathological evidence of steatohepatitis was also evident in HFD-fed mice, including macro- and micro-vesicular steatosis, marked hepatic inflammatory cell infiltration, and fibrosis in a majority of mice (Supplemental Figure 4). HFD-fed mice had increased fibrin degradation products (Figure 2C), indicating endogenous fibrin formation and lysis.

We then used these mice to test the hypothesis that HFD-induced obesity is associated with opposing changes in the kinetics of both TG and PG. Experiments were performed using low and high TF to mimic endothelial dysfunction associated with venous thrombosis and severe vascular injury such as that observed with plaque rupture, respectively.<sup>33</sup> Compared to CD, HFD did not alter the TG lagtime or TtPeak, but significantly increased the TG velocity at low TF and increased the peak and ETP at both low and high TF (Figure 3A-F). Analysis of PG revealed a different pattern. Compared to CD-fed mice, PG was significantly delayed (prolonged lagtime, TtPeak, and reduced velocity) in HFD-fed mice at both low and high TF, but no change in the plasmin peak was evident at either TF concentration (Figure 3G-K). HFD increased the EPP (Figure 3L). Similar results were observed for mice fed for 16 weeks and or with a higher fat diet (Supplemental Figure 5). Multiple PG parameters correlated significantly with body weight and serum ALT, especially in reactions triggered with low TF (Table 2), strongly associating the observed changes in PG with HFD.

The combined functional effects of HFD feeding on plasma clotting and fibrinolysis were revealed in turbidity assays in which plasmas from HFD-fed mice demonstrated normal fibrin formation kinetics but significantly delayed clot lysis (Figure 3M-R). Collectively, these findings suggest the effect of HFD on TG and PG kinetics culminates in fibrin formation that is not balanced by an appropriate fibrinolytic response.

**Changes in PAI-1 are insufficient to explain abnormalities in PG parameters in HFD-fed obese mice.** To identify the molecular mechanisms contributing to delayed PG in HFD-fed mice, we first measured the plasma concentrations of proteins already known to affect PG. Concentrations of fibrinogen, plasminogen, and  $\alpha_2$ -antiplasmin were not significantly different between CD- and HFD-fed mice (Figure 4A-C). Previous studies showed that expression of the endogenous tPA inhibitor PAI-1 strongly correlates with body mass index in obese humans and mice, and PAI-1 has an important role in venous thrombosis and resistance of platelet-rich arterial thrombi to lysis.<sup>15, 17, 19, 34</sup> PAI-1 is synthesized in an active form, but converts spontaneously to a latent (inactive) conformation in plasma, comprising ~90% of total circulating PAI-1.<sup>35</sup> To determine if delayed PG could be attributed to elevated PAI-1, we measured total and active PAI-1 in plasmas from CD- and HFD-fed mice. Compared to CD-fed mice, HFD-fed mice had increased total and active PAI-1 (Figure 4D-E), and these

correlated with body weight (Figure 4F-G) and multiple PG parameters (Table 3). To determine whether elevated PAI-1 in HFD-fed mice delays PG in the PG assay, we spiked normal plasma with mouse PAI-1 and measured PG. Increasing total PAI-1 did not prolong PG (Figure 4H). Spiking plasma with active human PAI-1 inhibited PG (Figure 4I); however, the concentration required to inhibit PG in this exogenous tPA-triggered assay was 100-fold higher than that detected in HFD-fed mice, suggesting the observed delay in PG stemmed from a second, independent antifibrinolytic mechanism.

**Elevated thrombomodulin and carboxypeptidase activity contribute to delayed PG.** To more broadly survey differences between CD- and HFD-fed mice that could contribute to delayed PG, we characterized the plasma proteomes from these mice using mass spectrometry. Using the Ward clustering algorithm with Euclidean distance measurements, the two groups were readily distinguished by relative protein levels (Figure 5A). Partial least squares discriminant analysis data reduction methods segregated plasmas from CD- and HFD-fed mice (Figure 5B). Differences between groups were driven largely by metabolic pathways. Analysis did not detect substantive post-translational modification of circulating fibrinogen in HFD-fed mice, but approximately 70 proteins were significantly ( $P \leq 0.05$ ) different between groups (Supplemental Table 1). As anticipated<sup>10</sup>, Kyoto Encyclopedia of Genes and Genomes (KEGG) analysis revealed significant enrichments in pathways associated with complement and coagulation ( $P < 10^{-12}$ ) and cholesterol metabolism ( $P < 10^{-8}$ ) (Figure 5C). In particular, HFD-fed mice showed significant elevations in two proteins with potential functions in fibrinolytic pathways: C-1-inhibitor and carboxypeptidase B2 (also known as the thrombin-activatable fibrinolysis inhibitor [TAFI]) (Figure 5D-E, respectively). C-1-inhibitor can inactivate fibrinolytic proteases including tPA and plasmin, whereas activated TAFI (TAFIa) cleaves C-lysine residues from fibrin, preventing tPA-mediated activation of plasminogen.<sup>36, 37</sup> Both C-1-inhibitor and TAFI correlated significantly with PG parameters (Supplemental Figure 6), and TAFI measurements confirmed by ELISA (Figure 5F) correlated significantly with data from mass spectrometry ( $R = 0.672$ ,  $P = 0.039$ ).

To determine the potential contribution of these proteins to PG, we spiked human C-1-inhibitor or zymogen human TAFI into plasma from wild-type mice and measured the effect on PG. Surprisingly, however, neither protein altered PG in this experiment (Figure 6A-B). Although TAFI can be activated by thrombin or plasmin, the thrombin/thrombomodulin complex substantially enhances TAFI activation (1250-fold).<sup>38-40</sup> Thrombomodulin is primarily membrane-bound, but elevated soluble thrombomodulin has been detected in plasmas from humans and mice with obesity or inflammatory disease.<sup>41-45</sup> Therefore, we tested the hypothesis that functional manifestations of elevated TAFI in HFD-fed mice are unveiled by low levels of endogenous

circulating thrombomodulin that were below the level of detection by mass spectrometry. Immunoblot analysis of plasmas from CD- and HFD-fed mice using CTM1009 antibody which recognizes the extracellular region of thrombomodulin revealed increased levels of a ~56 kDa band in HFD mice (Figure 6C-D). This band is smaller than full-length mouse thrombomodulin (~78 kDa<sup>46</sup>), suggesting it represents a cleaved form of thrombomodulin (*i.e.*, a species lacking the intracellular and transmembrane regions). Whereas band intensity did not correlate with TG lagtime, TtPeak, velocity, or peak (Supplemental Figure 7A-D), it correlated significantly with PG lagtime, TtPeak, velocity, and EPP (Supplemental Figure 7F-J).

To determine potential functional effects of soluble thrombomodulin on TG, PG, and fibrin formation/lysis, we spiked wild-type plasma with recombinant mouse thrombomodulin (rmTM). Addition of low concentrations of rmTM that had no effect on TG (Figure 6E) significantly delayed PG (Figure 6F) and clot lysis (Figure 6G), and addition of monoclonal anti-mouse thrombomodulin antibody (MTM-1701)<sup>47</sup> or potato tuber carboxypeptidase inhibitor (PTCI) to block carboxypeptidase activity reversed this effect (Figure 6F-H). Importantly, addition of MTM-1701 or PTCI shortened the PG lagtime and TtPeak and increased the velocity and peak in plasmas from both CD- and HFD-fed mice, and effects were more pronounced in HFD-fed mice (Figure 6I-O). Collectively, these data suggest PG is delayed in HFD-fed mice via thrombomodulin-dependent activation of a carboxypeptidase activity, that is likely TAFI.

**Prothrombotic phenotype can be detected in the relative kinetics of TG and PG.** Representative curves showing TG, PG, and combined effects on fibrin formation and lysis for CD- and HFD-fed mice are depicted in Figure 7A-B. Although the onset of TG, and consequently fibrin formation, was rapid in both CD- and HFD-fed mice, delayed PG in HFD-fed mice produced a substantial delay in clot lysis. To quantify the degree of malalignment between TG and PG in HFD-fed mice, we calculated the TG/PG ratio for each parameter. TG/PG ratios for TtPeak and velocity correlated significantly with body weight, whereas the TG/PG ratio for peak correlated significantly with serum ALT (Table 4), suggesting independent mechanisms mediate relationships between PG and body weight and liver function in HFD-fed mice. Compared to CD-fed mice, HFD-fed mice had abnormal TG/PG ratios for parameters coinciding with fibrin formation: lagtime, TtPeak, and velocity (Figure 7C-G). The degree of imbalance in these early parameters was not readily apparent from TG analysis alone, suggesting the TG/PG ratio reveals a global dysregulation in mechanisms that promote fibrin deposition and persistence. Collectively, these data suggest comprehensive assessment of procoagulant and fibrinolytic capacity provides unique insight into coagulopathic mechanisms caused by HFD in mice.

## DISCUSSION

A majority of research centered on perturbations in coagulation in obesity has focused on procoagulant factors in obese patients and related experimental settings. However, although abnormal concentrations of circulating proteins comprising the plasminogen activator system (e.g., tPA, plasminogen, PAI-1,  $\alpha_2$ -antiplasmin, TAFI) are also evident in obesity, the functional impact of these abnormalities has been difficult to define. Our development of a calibrated assay to measure PG kinetics in parallel with TG provides the opportunity to quantify the global imbalance of processes that normally control fibrin deposition and dissolution. Application of this assay uncovered a previously undescribed thrombomodulin- and TAFI-dependent delay in PG kinetics in a robust setting of experimental obesity.

Increased plasma concentrations of the tPA inhibitor, PAI-1 have been documented in prior studies of obese humans and mice, and PAI-1 has emerged as a potential target for antithrombotic therapy. Interestingly, the relative insensitivity of our exogenous tPA-driven PG assay to active PAI-1 enabled our discovery of a second hypofibrinolytic mechanism involving thrombomodulin. Following activation of coagulation, thrombin binding to thrombomodulin shifts its specificity from procoagulant (e.g., fibrin) to anticoagulant and profibrinolytic substrates (e.g., protein C and TAFI, respectively). The relative contribution of the thrombin/thrombomodulin complex to anticoagulant and antifibrinolytic pathways is determined by the thrombomodulin concentration. Whereas high thrombomodulin inhibits coagulation by promoting protein C activation, low concentrations of cellular or soluble thrombomodulin promote TAFI activation.<sup>38, 48</sup> TAFIa removes C-terminal lysine residues from fibrin, reducing binding sites for both plasmin and plasminogen.<sup>37</sup> Consequently, TAFIa decreases fibrin cleavage by plasmin as well as fibrin's ability to support PG. Although carboxypeptidase N (CPN) also possesses this activity and is inhibited by PTCL, CPN is constitutively active. TAFI requires activation by the thrombin-thrombomodulin complex or glycosaminoglycan-bound plasmin<sup>49</sup>, making it the likely effector in this setting. Thus, our findings suggest a mechanism in which HFD induces a functional increase in soluble thrombomodulin that is insufficient to inhibit TG, but which facilitates thrombin-mediated activation of TAFI. Since a previous study attributed hypofibrinolysis in plasma from obese children to both PAI-1 and TAFI<sup>50</sup>, these proteins likely function simultaneously but independently, resulting in potent antifibrinolytic activity in obesity.

Prior studies have detected low concentrations of soluble thrombomodulin in plasma from even healthy humans (292 ng/mL<sup>51</sup>). Accordingly, we observed thrombomodulin-dependent effects on PG in plasma from both CD- and HFD-fed mice; however, effects were enhanced by HFD. The source of, and mechanisms that

increase circulating thrombomodulin in obese humans and mice are unclear. Although thrombomodulin can be detected in leukocytes and platelets, it is predominantly expressed on vascular endothelium.<sup>52-54</sup> Consequently, thrombomodulin in plasma of patients with inflammatory disease or obesity likely originates from shedding of thrombomodulin from activated endothelium. Consistent with this premise, our analysis of the plasma proteome also revealed elevated biomarkers of activated endothelium in HFD-fed mice (e.g., von Willebrand factor [1.9-fold,  $P=0.015$ ] and soluble vascular cell adhesion molecule-1 [1.3-fold,  $P=0.097$ ], Supplemental Table 1). Specific mechanisms that increase thrombomodulin shedding in diet-induced obesity are unclear, but likely stem from inflammatory processes. Cytokines and adipokines associated with HFD, including tumor necrosis factor- $\alpha$  and leptin, reduce endothelial expression of thrombomodulin, but paradoxically increase thrombomodulin release into the circulation.<sup>43, 55-60</sup> Neutrophil-derived enzymes and oxidative damage also promote thrombomodulin shedding from endothelium.<sup>61</sup> Our proteomic analysis of plasma from HFD-fed mice revealed increased cathepsin B (1.9-fold,  $P=0.003$ ), which can enhance protease activity, and reduced glutathione peroxidase-3 (0.75-fold,  $P<0.005$ ), which protects against oxidative damage. Since thrombomodulin has diverse and pleiotropic effects in physiology, it is difficult to conclude whether shedding is a pathologic result of the HFD or a compensatory mechanism that limits HFD-associated pathologies. However, it appears that this shift in thrombomodulin compartmentalization away from the endothelium to the plasma decreases vessel wall-associated anticoagulant activity while simultaneously inhibiting fibrinolytic activity. The potential for additive or synergistic contributions of these mechanisms to HFD-driven obesity warrants further analysis.

Our results documenting delayed plasma PG in experimental obesity offer insight into the prothrombotic state accompanying metabolic disease. Previous studies have documented a reciprocal relationship between fibrin formation and obesity. Specifically, fibrin engagement of leukocyte  $\beta_2$  integrins drives adipose and hepatic inflammation, amplifying HFD-induced obesity and fatty liver disease.<sup>9, 62</sup> Reducing coagulation activation genetically or pharmacologically decreases fibrin deposition in adipose tissue and liver, and inhibits HFD-induced obesity in mice.<sup>9, 62</sup> Thus, cyclical amplification of obesity and its sequelae by thrombomodulin/TAFI-dependent inhibition of fibrinolysis may stabilize fibrin deposits that potentiate inflammation. This situation may be similar to mechanisms driving metabolic advantages of PAI-1-deficient mice, which are protected from obesity and insulin resistance.<sup>19, 63</sup> By extension, the thrombomodulin/TAFI-dependent antifibrinolytic pathway may represent a novel target to enhance fibrin dissolution and consequently, decrease fibrin-driven inflammation in obesity. Given the complex role of thrombomodulin in both anticoagulant and antifibrinolytic functions, thrombomodulin-directed therapies are likely untenable. Interestingly, however, increased circulating TAFI in obese humans and mice is correlated with

hypofibrinolysis and thrombotic risk.<sup>18, 64-67</sup> In vitro and in vivo studies show profibrinolytic effects from TAFI inhibition, including enhanced fibrinolysis in whole blood and plasma<sup>68-71</sup>, reduced FeCl<sub>3</sub> injury-induced vena cava thrombus mass in mice<sup>71, 72</sup>, and enhanced tPA-mediated thrombolysis in rabbits.<sup>73</sup> These effects may be achievable with minimal bleeding risk, insofar as TAFI-deficient mice do not have a hemorrhagic phenotype or exhibit increased bleeding following tail transection.<sup>74</sup> Proof-of-concept stems from studies successfully targeting thrombin/thrombomodulin-dependent TAFI activation to enhance fibrinolysis in a baboon model of sepsis<sup>75</sup>, another setting in which thrombomodulin transitions from endothelium to a soluble form in plasma.

Prior studies have reported methods to measure PG kinetics in plasma using fluorescent substrates.<sup>21-23</sup> Concentrations of TF and tPA differed modestly between these studies, ranging from ~0.28-5 pM TF and ~3.3-7.5 nM tPA, but were similar to concentrations used in our study (0.5 pM TF and ~5.2 nM tPA). However, these methods had potential caveats, including active plasmin trapped by  $\alpha_2$ M that can still cleave the fluorogenic substrate, inner filter effects, and use of solvents that may compromise fibrin formation. Advances of our assay include the use of a mathematical model to correct for substrate consumption and the inner filter effect<sup>76</sup>, calibration with  $\alpha_2$ M-Pm complex, and a water-soluble fluorogenic substrate. Although the use of diluted plasma may alter some biochemical relationships, dilution reduces substrate consumption<sup>77</sup>, enables direct comparison to TG values<sup>24</sup>, and also solves logistical problems of small sample volumes in mouse studies. Our PG assay is triggered by human TF and tPA because mouse proteins are not as readily available. Human tPA exhibits similar dose-dependent binding to mouse fibrin as mouse tPA<sup>78</sup>, and like mouse tPA, is rapidly inhibited by both human and mouse PAI-1, yielding similar  $t_{1/2}$  in mouse plasma.<sup>78</sup> In the absence of fibrin, activation of mouse plasminogen by human tPA is ~200-fold lower than by mouse tPA; however, in the presence of fibrin, it is only 5-10-fold lower<sup>78</sup>, making the PG assay quite sensitive to fibrin's cofactor activity in mouse plasma.<sup>29</sup> It is therefore interesting to speculate that if applied to other models of disease, the PG assay could also detect abnormalities in fibrinogen synthesis or post-translational modifications (e.g., acetylation, glycation, and homocysteinylation) that have been associated with abnormal fibrinolysis.<sup>79-82</sup> For example, use of our assay to differentiate effects of these modifications on abnormal fibrin structure versus defective PG may provide insight into the underlying pathophysiology in diseases including atherosclerosis and diabetes. In addition, since the rtPA concentrations we used are within levels targeted during therapeutic thrombolysis, the PG assay may inform studies of thrombus treatment or resolution.

Readouts from our PG assay may provide quantitative measures to define coagulopathy in pathological settings. First, use of a TG/PG ratio may yield a metric to identify global dysregulation in the mechanisms regulating these processes, as well as situations in which "rebalancing" has occurred. A classic example is liver

dysfunction, in which multiple plasma proteins are altered simultaneously and phenotypes are difficult to predict.<sup>83</sup> Differences between CD- and HFD-fed mice were significant at both low and high TF concentrations, suggesting both mild and severe events that expose TF to blood (e.g., endothelial activation and plaque rupture) may promote robust and stable fibrin deposition. Second, in studies of thrombotic disease, integration of ex vivo measures of coagulation (e.g., TAT, F1+2) with TG parameters provides complementary information on ongoing coagulation events in vivo and residual procoagulant potential in plasma. Measurements of fibrinolysis end-products (e.g., PAP, D-dimer) with plasma PG may similarly be used to assess fibrinolytic events in vivo in concert with remaining fibrinolytic potential. Moreover, integration of procoagulant and fibrinolytic measurements may be used to define overall capacity to generate and sustain fibrin not only in obesity, but also in other settings involving simultaneous dysregulation of coagulation and fibrinolytic systems, including infection and disseminated intravascular coagulation.

In summary, we report a new PG assay and its application to an experimental model of diet-induced obesity in mice. Our analysis documents a hemostatic imbalance in different HFDs and durations of feeding and exposes the antifibrinolytic activity of soluble thrombomodulin and thrombomodulin-activated TAFI. Discovery of this mechanism has functional consequences beyond intravascular thrombus formation, as this pathway may permit the persistence of fibrin that drives metabolic disease. It remains unclear whether changes in PG result from HFD, manifestations of obesity, or both. It will be interesting to determine whether abnormal PG can be detected in genetic models of obesity and in obese humans, and whether the TG/PG ratio can be used to differentiate the so-called ‘healthy obese.’ Since elevated thrombomodulin has been detected in plasma from patients with other proinflammatory and prothrombotic diseases including cardioembolic stroke<sup>41</sup>, sepsis-associated disseminated intravascular coagulation<sup>42</sup>, and atherosclerosis<sup>45</sup>, the antifibrinolytic mechanism unearthed here may have broad relevance across a range of inflammatory settings.

## ACKNOWLEDGEMENTS

The authors thank Dr. Charles T. Esmon for providing antibodies and Dr. Robert A. Campbell for reading the manuscript.

## FUNDING

This study was supported by funding from the National Institutes of Health (R61HL141791 to ASW, U01HL143403 to ASW and MJF, R01ES017537 to JPL, and R01DK112778 to MJF).

## **AUTHORSHIP**

AM, BdL, and ASW developed the hypothesis; AM, AKK, AP, KCH, LAH, and JRB performed experiments and/or collected data; VAP, FJC, and DAL provided essential reagents; AM, KCH, MJF, JPL, and ASW analyzed data; AM, JPL, and ASW interpreted data; AM, MJF, JPL, and ASW wrote the manuscript, which was revised and approved by all authors.

## **CONFLICT OF INTEREST DISCLOSURE**

AM and BdL are employed by Synapse Research Institute, a member of the STAGO Diagnostic group that produces calibrated automated thrombography for thrombin generation measurements in plasma. None of the other authors have relevant potential conflict of interest.

## **DATA SHARING**

For original data, please contact the corresponding author.

## REFERENCES

1. Blüher M. Obesity: global epidemiology and pathogenesis. *Nat Rev Endocrinology*. 2019;15:288-298.
2. Targher G, Bertolini L, Padovani R, Rodella S, Tessari R, Zenari L, Day C and Arcaro G. Prevalence of nonalcoholic fatty liver disease and its association with cardiovascular disease among type 2 diabetic patients. *Diabetes Care*. 2007;30:1212-1218.
3. Kernan WN, Inzucchi SE, Sawan C, Macko RF and Furie KL. Obesity: a stubbornly obvious target for stroke prevention. *Stroke*. 2013;44:278-286.
4. Abdollahi M, Cushman M and Rosendaal FR. Obesity: risk of venous thrombosis and the interaction with coagulation factor levels and oral contraceptive use. *Thromb Haemost*. 2003;89:493-498.
5. Mitchell AB, Cole JW, McArdle PF, Cheng Y-C, Ryan KA, Sparks MJ, Mitchell BD and Kittner SJ. Obesity increases risk of ischemic stroke in young adults. *Stroke*. 2015;46:1690-1692.
6. Mertens I and Gaal LFV. Obesity, haemostasis and the fibrinolytic system. *Obes Rev*. 2002;3:85-101.
7. Kotronen A, Joutsu-Korhonen L, Sevastianova K, Bergholm R, Hakkarainen A, Pietiläinen KH, Lundbom N, Rissanen A, Lassila R and Yki-Järvinen H. Increased coagulation factor VIII, IX, XI and XII activities in non-alcoholic fatty liver disease. *Liver Int*. 2011;31:176-183.
8. Kaye SM, Pietiläinen KH, Kotronen A, Joutsu-Korhonen L, Kaprio J, Yki-Jarvinen H, Silveira A, Hamsten A, Lassila R and Rissanen A. Obesity-related derangements of coagulation and fibrinolysis: A study of obesity-discordant monozygotic twin pairs. *Obesity*. 2012;20:88-94.
9. Kopec AK, Abrahams SR, Thornton S, Palumbo JS, Mullins ES, Divanovic S, Weiler H, Owens AP, III, Mackman N, Goss A, van Ryn J, Luyendyk JP and Flick MJ. Thrombin promotes diet-induced obesity through fibrin-driven inflammation. *J Clin Invest*. 2017;127:3152-3166.
10. Geyer PE, Wewer Albrechtsen NJ, Tyanova S, Grassl N, Iepsen EW, Lundgren J, Madsbad S, Holst JJ, Torekov SS and Mann M. Proteomics reveals the effects of sustained weight loss on the human plasma proteome. *Molecular Systems Biology*. 2016;12:901-917.
11. Vilahur G, Ben-Aicha S and Badimon L. New insights into the role of adipose tissue in thrombosis. *Cardiovascular Research*. 2017;113:1046-1054.
12. Tripodi A. Thrombin generation assay and its application in the clinical laboratory. *Clin Chem*. 2016;62:699-707.

13. Ay L, Kopp H-P, Brix J-M, Ay C, Quehenberger P, Schernthaner G-H, Pabinger I and Schernthaner G. Thrombin generation in morbid obesity: significant reduction after weight loss. *J Thromb Haemost.* 2010;8:759-765.
14. Chitongo PB, Roberts LN, Yang L, Patel RK, Lyall R, Luxton R, Aylwin SJB and Arya R. Visceral adiposity is an independent determinant of hypercoagulability as measured by thrombin generation in morbid obesity. *TH Open.* 2017;01:e146-e154.
15. Targher G, Bertolini L, Scala L, Zenari L, Lippi G, Franchini M and Arcaro G. Plasma PAI-1 levels are increased in patients with nonalcoholic steatohepatitis. *Diabetes Care.* 2007;30:e31-e32.
16. Lijnen HR. Role of fibrinolysis in obesity and thrombosis. *Thromb Res.* 2009;123:S46-S49.
17. Juhan-Vague I and Alessi MC. PAI-1, obesity, insulin resistance and risk of cardiovascular events. *Thromb Haemost.* 1997;78:656-660.
18. Hori Y, Gabazza EC, Yano Y, Katsuki A, Suzuki K, Adachi Y and Sumida Y. Insulin resistance is associated with increased circulating level of thrombin-activatable fibrinolysis inhibitor in type 2 diabetic patients. *J Clin Endocrinol Metab.* 2002;87:660-665.
19. Ma L-J, Mao S-L, Taylor KL, Kanjanabuch T, Guan Y, Zhang Y, Brown NJ, Swift LL, McGuinness OP, Wasserman DH, Vaughan DE and Fogo AB. Prevention of obesity and insulin resistance in mice lacking plasminogen activator inhibitor 1. *Diabetes.* 2004;53:336-346.
20. Balagopal P, Mann KJ, Sweeten S and George D. Effect of obesity and physical activity on D-dimer – A Randomized controlled study in Adolescents. *FASEB J.* 2008;22:880-881.
21. Van Geffen M, Loof A, Lap P, Boezeman J, Laros-van Gorkom BAP, Brons P, Verbruggen B, Kraaij Mv and Van Heerde WL. A novel hemostasis assay for the simultaneous measurement of coagulation and fibrinolysis. *Hematology.* 2011;16:327-336.
22. Matsumoto T, Nogami K and Shima M. Simultaneous measurement of thrombin and plasmin generation to assess the interplay between coagulation and fibrinolysis. *Thromb Haemost.* 2013;110:761-768.
23. Simpson ML, Goldenberg NA, Jacobson LJ, Bombardier CG, Hathaway WE and Manco-Johnson MJ. Simultaneous thrombin and plasmin generation capacities in normal and abnormal states of coagulation and fibrinolysis in children and adults. *Thromb Res.* 2011;127:317-323.
24. Tchaikovski SN, Van Vlijmen BJM, Rosing J and Tans G. Development of a calibrated automated thrombography based thrombin generation test in mouse plasma. *J Thromb Haemost.* 2007;5:2079-2086.

25. Bloemen S, Huskens D, Konings J, Kremers RM, Miszta A, de Laat B and Kelchtermans H. Interindividual variability and normal ranges of whole blood and plasma thrombin generation. *J Appl Lab Med*. 2017;2:150-164.
26. Honjo K, Munakata S, Tashiro Y, Salama Y, Shimazu H, Eiamboonsert S, Dhahri D, Ichimura A, Dan T, Miyata T, Takeda K, Sakamoto K, Hattori K and Heissig B. Plasminogen activator inhibitor-1 regulates macrophage-dependent postoperative adhesion by enhancing EGF-HER1 signaling in mice. *The FASEB Journal*. 2017;31:2625-2637.
27. Zhou H, Wu X, Lu X, Chen G, Ye X and Huang J. Evaluation of plasma urokinase-type plasminogen activator and urokinase-type plasminogen-activator receptor in patients with acute and chronic hepatitis B. *Thrombosis Research*. 2009;123:537-542.
28. Pieters M and Wolberg AS. Fibrinogen and fibrin: An illustrated review. *Res Pract Thromb Haemost*. 2019;3:161-172.
29. Medved L and Nieuwenhuizen W. Molecular mechanisms of initiation of fibrinolysis by fibrin. *Thromb Haemost*. 2003;89:409-419.
30. Prasad JM, Gorkun OV, Raghu H, Thornton S, Mullins ES, Palumbo JS, Ko Y-P, Höök M, David T, Coughlin SR, Degen JL and Flick MJ. Mice expressing a mutant form of fibrinogen that cannot support fibrin formation exhibit compromised antimicrobial host defense. *Blood*. 2015;126:2047-2058.
31. Wolberg AS. Thrombin generation and fibrin clot structure. *Blood Rev*. 2007;21:131-142.
32. Bannish BE, Chernysh IN, Keener JP, Fogelson AL and Weisel JW. Molecular and Physical Mechanisms of Fibrinolysis and Thrombolysis from Mathematical Modeling and Experiments. *Scientific Reports*. 2017;7:6914-6925.
33. Wolberg AS, Aleman MM, Leiderman K and Machlus KR. Procoagulant activity in hemostasis and thrombosis: Virchow's triad revisited. *Anesthesia and analgesia*. 2012;114:275-285.
34. Nagai N, Hoylaerts MF, Cleuren ACA, Van Vlijmen BJM and Lijnen HR. Obesity promotes injury induced femoral artery thrombosis in mice. *Thromb Res*. 2008;122:549-555.
35. Hekman CM and Loskutoff DJ. Endothelial cells produce a latent inhibitor of plasminogen activators that can be activated by denaturants. *J Biol Chem*. 1985;260:11581-11587.
36. Brown EW, Ravindran S and Patston PA. The reaction between plasmin and C1-inhibitor results in plasmin inhibition by the serpin mechanism. *Blood Coagul Fibrinolysis*. 2002;13:711-714.
37. Wang W, Boffa PB, Bajzar L, Walker JB and Nesheim ME. A study of the mechanism of inhibition of fibrinolysis by activated thrombin-activable fibrinolysis inhibitor. *J Biol Chem*. 1998;273:27176-27181.

38. Bajzar L, Morser J and Nesheim M. TAFI, or plasma procarboxypeptidase B, couples the coagulation and fibrinolytic cascades through the thrombin-thrombomodulin complex. *J Biol Chem.* 1996;271:16603-16608.
39. Boffa MB, Wang W, Bajzar L and Nesheim ME. Plasma and recombinant thrombin-activable fibrinolysis inhibitor (TAFI) and activated TAFI compared with respect to glycosylation, thrombin/thrombomodulin-dependent activation, thermal stability, and enzymatic properties. *J Biol Chem.* 1998;273:2127-2135.
40. Wang W, Nagashima M, Schneider M, Morser J and Nesheim M. Elements of the primary structure of thrombomodulin required for efficient thrombin-activable fibrinolysis inhibitor activation. *J Biol Chem.* 2000;275:22942-22947.
41. Dharmasaroja P, Dharmasaroja PA and Sobhon P. Increased plasma soluble thrombomodulin levels in cardioembolic stroke. *Clin Appl Thromb Hemost.* 2012;18:289-293.
42. Lin S-M, Wang Y-M, Lin H-C, Lee K-Y, Huang C-D, Liu C-Y, Wang C-H and Kuo H-P. Serum thrombomodulin level relates to the clinical course of disseminated intravascular coagulation, multiorgan dysfunction syndrome, and mortality in patients with sepsis. *Crit Care Med.* 2008;36:683-689.
43. Porreca E, Di Febbo C, Fusco L, Moretta V, Di Nisio M and Cuccurullo F. Soluble thrombomodulin and vascular adhesion molecule-1 are associated to leptin plasma levels in obese women. *Atherosclerosis.* 2004;172:175-180.
44. Rega-Kaun G, Kaun C, Ebenbauer B, Jaegersberger G, Prager M, Wojta J and Hohensinner PJ. Bariatric surgery in morbidly obese individuals affects plasma levels of protein C and thrombomodulin. *J Thromb Thrombolysis.* 2019;47:51-56.
45. Pawlak K, Mysliwiec M and Pawlak D. Kynurenine pathway – a new link between endothelial dysfunction and carotid atherosclerosis in chronic kidney disease patients. *Adv Med Sci.* 2010;55:196-203.
46. Weiler-Guettler H, Christie PD, Beeler DL, Healy AM, Hancock WW, Rayburn H, Edelberg JM and Rosenberg RD. A targeted point mutation in thrombomodulin generates viable mice with a prethrombotic state. *The Journal of Clinical Investigation.* 1998;101:1983-1991.
47. Lopez-Ramirez MA, Pham A, Girard R, Wyseure T, Hale P, Yamashita A, Koskimäki J, Polster S, Saadat L, Romero IA, Esmon CT, Lagarrigue F, Awad IA, Mosnier LO and Ginsberg MH. Cerebral cavernous malformations form an anticoagulant vascular domain in humans and mice. *Blood.* 2019;133:193-204.
48. Mosnier LO, Meijers JCM and Bouma BN. Regulation of fibrinolysis in plasma by TAFI and protein C is dependent on the concentration of thrombomodulin. *Thromb Haemost.* 2001;85:5-11.

49. Leung LLK and Morser J. Carboxypeptidase B2 and carboxypeptidase N in the crosstalk between coagulation, thrombosis, inflammation, and innate immunity. *Journal of Thrombosis and Haemostasis*. 2018;16:1474-1486.
50. Semeraro F, Giordano P, Faienza MF, Cavallo L, Semeraro N and Colucci M. Evidence that fibrinolytic changes in paediatric obesity translate into a hypofibrinolytic state. *Thromb Haemost*. 2012;108:311-317.
51. Ishii H and Majerus PW. Thrombomodulin is present in human plasma and urine. *J Clin Invest*. 1985;76:2178-2181.
52. Suzuki K, Nishioka J, Hayashi T and Kosaka Y. Functionally active thrombomodulin is present in human platelets. *J Biochem*. 1988;104:628-632.
53. Dittman W and Majerus P. Structure and function of thrombomodulin: a natural anticoagulant. *Blood*. 1990;75:329-336.
54. Conway E, Nowakowski B and Steiner-Mosonyi M. Human neutrophils synthesize thrombomodulin that does not promote thrombin-dependent protein C activation. *Blood*. 1992;80:1254-1263.
55. Nawroth PP, Handley DA, Esmon CT and Stern DM. Interleukin 1 induces endothelial cell procoagulant while suppressing cell-surface anticoagulant activity. *Proc Natl Acad Sci*. 1986;83:3460-3464.
56. Nawroth PP and Stern DM. Modulation of endothelial cell hemostatic properties by tumor necrosis factor. *J Exp Med*. 1986;163:740-745.
57. Hotamisligil G, Shargill N and Spiegelman B. Adipose expression of tumor necrosis factor-alpha: direct role in obesity-linked insulin resistance. *Science*. 1993;259:87-91.
58. Boehme MW, Deng Y, Raeth U, Bierhaus A, Ziegler R, Stremmel W and Nawroth PP. Release of thrombomodulin from endothelial cells by concerted action of TNF-alpha and neutrophils: in vivo and in vitro studies. *Immunology*. 1996;87:134-140.
59. Maruyama I, Nakata M and Yamaji K. Effect of leptin in platelet and endothelial cells: obesity and arterial thrombosis. *Ann N Y Acad Sci*. 2000;902:315-319.
60. Sohn RH, Deming CB, Johns DC, Champion HC, Bian C, Gardner K and Rade JJ. Regulation of endothelial thrombomodulin expression by inflammatory cytokines is mediated by activation of nuclear factor-kappa B. *Blood*. 2005;105:3910-3917.
61. Boehme MWJ, Galle P and Stremmel W. Kinetics of thrombomodulin release and endothelial cell injury by neutrophil-derived proteases and oxygen radicals. *Immunology*. 2002;107:340-349.

62. Luyendyk JP, Sullivan BP, Guo GL and Wang R. Tissue factor-deficiency and protease activated receptor-1-deficiency reduce inflammation elicited by diet-induced steatohepatitis in mice. *Am J Pathol.* 2010;176:177-186.
63. Lijnen HR, Maquoi E, Morange P, Voros G, Hoef BV, Kopp F, Collen D, Juhan-Vague I and Alessi M-C. Nutritionally induced obesity is attenuated in transgenic mice overexpressing plasminogen activator inhibitor-1. *Arterioscler Thromb Vasc Biol.* 2003;23:78-84.
64. Mosnier LO, Von dem Borne PAK, Meijers JCM and Bouma BN. Plasma TAFI levels influence the clot lysis time in healthy individuals in the presence of an intact intrinsic pathway of coagulation. *Thromb Haemost.* 1998;80:829-835.
65. van Tilburg NH, Rosendaal FR and Bertina RM. Thrombin activatable fibrinolysis inhibitor and the risk for deep vein thrombosis. *Blood.* 2000;95:2855-2859.
66. Juhan-Vague I, Morange PE, Aubert H, Henry M, Aillaud MF and Alessi MC. Plasma thrombin-activatable fibrinolysis inhibitor antigen concentration and genotype in relation to myocardial infarction in the north and south of Europe. *Arterioscler Thromb Vasc Biol.* 2002;22:867-873.
67. Meltzer ME, Lisman T, de Groot PG, Meijers JCM, le Cessie S, Doggen CJM and Rosendaal FR. Venous thrombosis risk associated with plasma hypofibrinolysis is explained by elevated plasma levels of TAFI and PAI-1. *Blood.* 2010;116:113-121.
68. Marx PF, Wagenaar GTM, Reijerkerk A, Tiekstra MJ, van Rossum AGSH, Gebbink MFBG and Meijers JCM. Characterization of mouse thrombin-activatable fibrinolysis inhibitor. *Thromb Haemost.* 2000;83:297-303.
69. Gils A, Ceresa E, Macovei AM, Marx PF, Peeters M, Compernelle G and DeClerck PJ. Modulation of TAFI function through different pathways – implications for the development of TAFI inhibitors. *J Thromb Haemost.* 2005;3:2745-2753.
70. Hillmayer K, Macovei A, Pauwels D, Compernelle G, DeClerck PJ and Gils A. Characterization of rat thrombin-activatable fibrinolysis inhibitor (TAFI) – a comparative study assessing the biological equivalence of rat, murine and human TAFI. *J Thromb Haemost.* 2006;4:2470-2477.
71. Wang X, Smith PL, Hsu M-Y, Ogletree ML and Schumacher WA. Murine model of ferric chloride-induced vena cava thrombosis: evidence for effect of potato carboxypeptidase inhibitor. *J Thromb Haemost.* 2006;4:403-410.

72. Wang X, Smith PL, Hsu M-Y, Tamasi JA, Bird E and Schumacher WA. Deficiency in thrombin-activatable fibrinolysis inhibitor (TAFI) protected mice from ferric chloride-induced vena cava thrombosis. *J Thromb Thrombolysis*. 2007;23:41-49.
73. Nagashima M, Werner M, Wang M, Zhao L, Light DR, Pagila R, Morser J and Verhallen P. An inhibitor of activated thrombin-activatable fibrinolysis inhibitor potentiates tissue-type plasminogen activator-induced thrombolysis in a rabbit jugular vein thrombolysis model. *Thromb Res*. 2000;98:333-342.
74. Nagashima M, Yin ZF, Zhao L, White K, Zhu Y, Lasky N, Halks-Miller M, Broze GJ, Fay WP and Morser J. Thrombin-activatable fibrinolysis inhibitor (TAFI) deficiency is compatible with murine life. *J Clin Invest*. 2002;109:101-110.
75. Binette TM, Taylor FB, Peer G and Bajzar L. Thrombin-thrombomodulin connects coagulation and fibrinolysis: more than an in vitro phenomenon. *Blood*. 2007;110:3168-3175.
76. Hemker HC and Kremers R. Data management in thrombin generation. *Thromb Res*. 2013;131:3-11.
77. Smedt ED, Wagenvoord R and Hemker CH. The technique of measuring thrombin generation with fluorogenic substrates: 3. The effects of sample dilution. *Thromb Haemost*. 2009;101:165-170.
78. Lijnen HR, Van Hoef B, Beelen V and Collen D. Characterization of the murine plasma fibrinolytic system. *Eur J Biochem*. 1994;224:863-871.
79. Svensson J, Bergman A-C, Adamson U, Blombäck M, Wallén H and Jörneskog G. Acetylation and glycation of fibrinogen in vitro occur at specific lysine residues in a concentration dependent manner: A mass spectrometric and isotope labeling study. *Biochem Biophys Res Commun*. 2012;421:335-342.
80. Ajjan RA, Gamlen T, Standeven KF, Mughal S, Hess K, Smith KA, Dunn EJ, Anwar MM, Rabbani N, Thornalley PJ, Philippou H and Grant PJ. Diabetes is associated with posttranslational modifications in plasminogen resulting in reduced plasmin generation and enzyme-specific activity. *Blood*. 2013;122:134-142.
81. Gugliucci A, Menini T and Stahl AJC. Glycation of fibrinogen in diabetic patients: a practical colorimetric assay. *Glycosylation & Disease*. 1994;1:177-183.
82. Pieters M, van Zyl DG, Rheeder P, Jerling JC, Loots DT, van der Westhuizen FH, Gottsche LT and Weisel JW. Glycation of fibrinogen in uncontrolled diabetic patients and the effects of glycaemic control on fibrinogen glycation. *Thromb Res*. 2007;120:439-446.
83. Lisman T and Stravitz RT. Rebalanced hemostasis in patients with acute liver failure. *Semin Thromb Hemost*. 2015;41:468-473.

## TABLES

**Table 1. Intra-assay, inter-assay, and inter-mouse variation of plasmin generation parameters.**

Plasma Dilution	Lagtime (min)	TtPeak (min)	Velocity (nM/min)	Peak (nM)	EPP (nM×min)
<b>1:3</b>					
Intra-assay (N=7)	2.3±0.0 (0.0)	4.6±0.1 (2.8)	62.6±1.7 (2.7)	146.2±3.9 (2.7)	809±22 (2.7)
Inter-assay (N=4)	1.5±0.4 (24.9)	4.1±0.5 (12.3)	67.4±8.3 (12.4)	166.0±11.5 (6.9)	964±33 (3.6)
Inter-mouse (N=6)	2.4±0.2 (5.9)	4.8±0.2 (3.5)	57.2±8.0 (14.0)	151.3±17.4 (11.5)	888±82 (9.3)
<b>1:6</b>					
Intra-assay (N=7)	2.3±0.0 (0.0)	4.3±0.0 (0.0)	51.9±3.2 (6.2)	103.1±6.4 (6.2)	444±24 (5.5)
Inter-assay (N=4)	1.9±0.3 (16.5)	3.7±0.5 (13.4)	49.7±8.0 (16.1)	115.1±9.6 (8.3)	586±95 (16.2)
Inter-mouse (N=6)	1.9±0.2 (8.8)	3.9±0.3 (7.1)	52.6±4.3 (8.2)	104.8±11.1 (10.6)	484±83 (17.0)

Plasmin generation was performed at 1 pM TF, 4 μM phospholipids, and 1.25 μg/mL rtPA. Mean ± standard deviation (% coefficient of variation)

**Table 2. Correlations between plasmin generation parameters and body weight and serum ALT in mice.**

	TF (pM)	Lagtime (min)	TtPeak (min)	Velocity (nM/min)	Peak (nM)	EPP (nM×min)
<b>Body Weight (g)</b>						
0.5	0.607 (0.069)	<b>0.838 (0.004)</b>	<b>-0.793 (0.009)</b>	0.333 (0.348)	<b>0.830 (0.004)</b>	
2	0.636 (0.053)	<b>0.650 (0.046)</b>	-0.563 (0.096)	0.103 (0.785)	0.381 (0.278)	
<b>Serum ALT (U/mL)</b>						
0.5	<b>0.779 (0.011)</b>	<b>0.838 (0.004)</b>	<b>-0.830 (0.004)</b>	0.551 (0.105)	<b>0.975 (&lt;0.001)</b>	
2	<b>0.672 (0.037)</b>	<b>0.656 (0.044)</b>	-0.612 (0.066)	-0.127 (0.733)	0.539 (0.114)	

Spearman correlation coefficient [R (*P* value)]

**Table 3. Correlations between plasmin generation parameters and PAI-1 in mice.**

	TF (pM)	Lagtime (min)	TtPeak (min)	Velocity (nM/min)	Peak (nM)	EPP (nM×min)
<b>Total PAI-1 (ng/mL)</b>						
0.5	<b>0.730 (0.021)</b>	<b>0.911 (&lt;0.001)</b>	<b>-0.866 (0.002)</b>	0.430 (0.218)	<b>0.927 (&lt;0.001)</b>	
2	<b>0.758 (0.014)</b>	<b>0.759 (0.013)</b>	<b>-0.660 (0.043)</b>	-0.151 (0.682)	0.503 (0.144)	
<b>Active PAI-1 (ng/mL)</b>						
0.5	<b>0.656 (0.046)</b>	<b>0.766 (0.013)</b>	<b>-0.842 (0.003)</b>	0.381 (0.278)	<b>0.830 (0.005)</b>	
2	0.623 (0.059)	<b>0.686 (0.032)</b>	-0.550 (0.105)	-0.248 (0.492)	0.430 (0.218)	

Spearman correlation coefficient [R (*P* value)]

**Table 4. Correlations between TG/PG ratios and body weight and serum ALT in mice.**

	TF (pM)	Lagtime (min)	TtPeak (min)	Velocity (nM/min)	Peak (nM)	EPP (nM×min)
Body Weight (g)						
	0.5	-0.474 (0.168)	<b>-0.697 (0.031)</b>	0.576 (0.088)	0.612 (0.067)	0.030 (0.946)
	2	-0.480 (0.162)	-0.564 (0.096)	0.588 (0.081)	0.321 (0.368)	0.127 (0.733)
Serum ALT (U/mL)						
	0.5	<b>-0.815 (0.006)</b>	<b>-0.855 (0.003)</b>	<b>0.685 (0.035)</b>	0.636 (0.054)	0.333 (0.349)
	2	<b>-0.760 (0.014)</b>	<b>-0.697 (0.031)</b>	0.624 (0.060)	0.624 (0.060)	0.236 (0.514)

Spearman correlation coefficient [R (*P* value)].

## FIGURE LEGENDS

**Figure 1. Characterization of plasmin generation (PG) assay.** (A) Platelet-poor plasma was mixed with tissue factor (TF), phospholipids, and recombinant tissue plasminogen activator (rtPA). Calibrator wells contained plasma and calibrator ( $\alpha_2$ -macroglobulin/plasmin complex). Reactions were initiated by automatically dispensing fluorogenic substrate and  $\text{CaCl}_2$  to each well. These reactions produced two fluorescence curves (raw fluorescence from plasmin generation in plasma in black, calibrator curve in dashed line) from which a PG curve was derived and associated parameters were calculated: time to plasmin generation (lagtime), time to peak (TtPeak), velocity, maximum plasmin concentration produced (peak), and time integral of PG (endogenous plasmin potential, EPP). (B) PG was measured in  $Plg^{+/+}$  and  $Plg^{-/-}$  plasmas diluted 1:6 (N=3 mice/group); averaged curves are shown. (C-D) PG was measured in normal, pooled plasma (diluted 1:6) in the presence of (C) 1.25  $\mu\text{g/mL}$  or (D) 0.31  $\mu\text{g/mL}$  rtPA, with increasing concentrations of  $\alpha_2$ -antiplasmin ( $\alpha_2$ -AP, note longer time scale in D). (E) PG was measured in normal, pooled plasma diluted in HEPES-buffered saline. Dilutions are indicated as plasma-to-buffer ratio. (F-G) Normal, pooled plasma was diluted (F) 1:3 or (G) 1:6 and PG was measured in the presence of the indicated concentrations of rtPA. (H-P) Thrombin generation, fibrin formation, and PG were measured in 1:6 diluted plasmas from littermate-matched wild-type mice and: (H-J) fibrinogen-deficient mice ( $Fga^{+/-}$ ,  $Fga^{-/-}$ ), (K-M) mice expressing mutated fibrinogen that cannot polymerize ( $Fgn^{AEK}$ ), and (N-P) factor XIII-deficient mice ( $F13a1^{+/-}$ ,  $F13a1^{-/-}$ ), or (Q-S) different TF concentrations (0.05-6 pM). All reactions included 1 pM TF and 1.25  $\mu\text{g/mL}$  rtPA unless otherwise indicated. Panels C-S, show representative curves.

**Figure 2. HFD leads to obesity and increased circulating fibrin degradation products.** Mice were fed for 12 weeks with a control diet (CD) or a high fat diet (HFD) (N=5/group). (A) Mean body weight, \* $P < 0.05$  and \*\* $P < 0.01$ . (B) Serum alanine aminotransferase (ALT) and (C) plasma fibrin degradation products; bars indicate medians, each dot represents a separate mouse.

**Figure 3. HFD increases thrombin generation (TG) and delays plasmin generation (PG) and fibrinolysis.** (A-F) TG and (G-L) PG for CD- and HFD-fed mice were measured in the presence of 0.5 and 2 pM TF and 0.31  $\mu\text{g/mL}$  rtPA (for PG assays). (M-R) Turbidity was measured in the presence of 0.5 pM TF and 0.31  $\mu\text{g/mL}$  rtPA. Panels A, G, and M show representative curves. Bars indicate medians. Each dot represents a separate mouse.

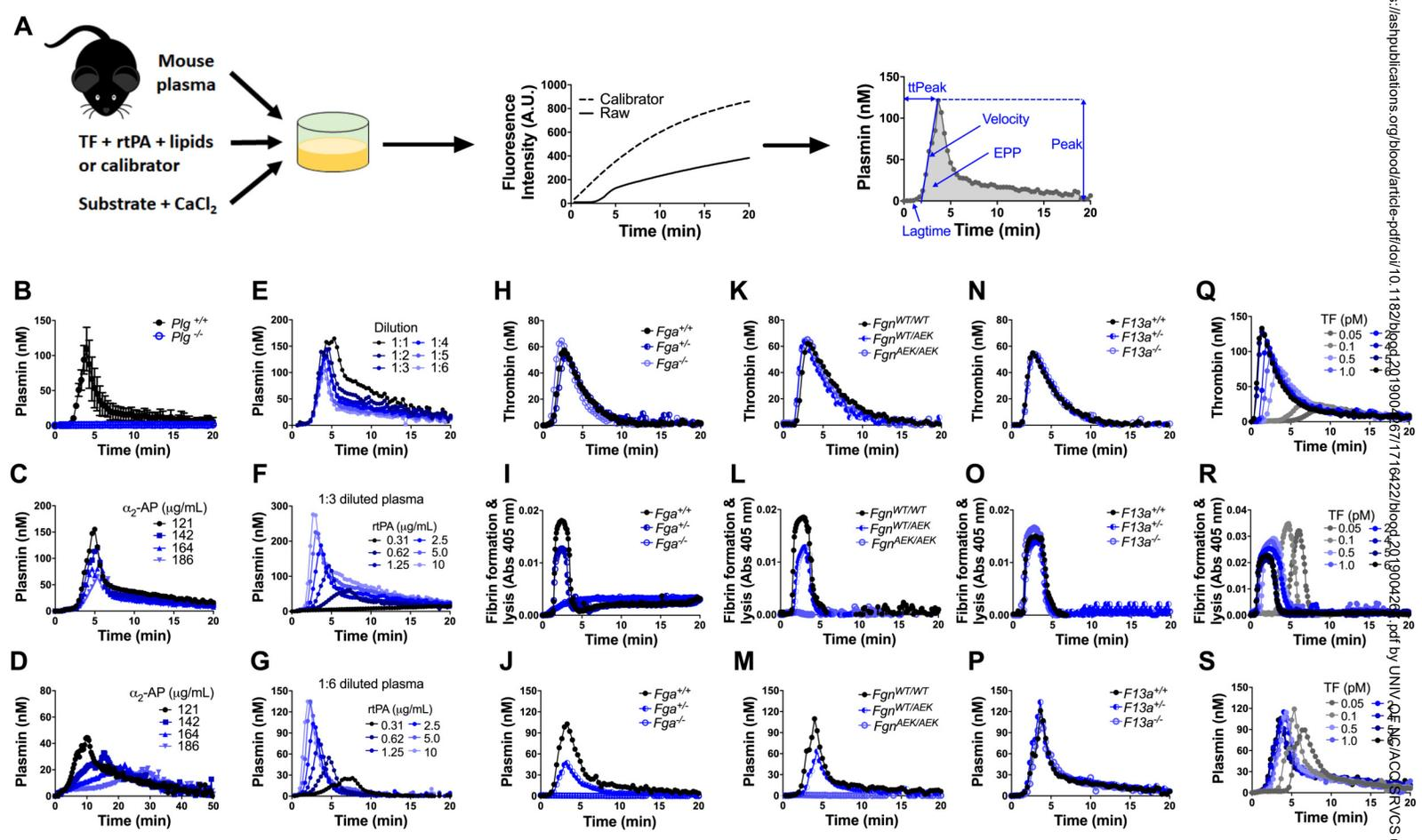
**Figure 4. Increased PAI-1 is not sufficient to explain delayed PG in HFD-fed mice.** (A) Fibrinogen, (B) plasminogen, (C)  $\alpha_2$ -antiplasmin, (D) total PAI-1, and (E) active PAI-1 in plasma from CD- and HFD-fed mice. Fibrinogen was measured by immunoblot and densitometry to confirm presence of all 3 chains;  $\beta$ -chain was used for quantification. Plasminogen,  $\alpha_2$ -antiplasmin, and PAI-1 were measured by ELISA. (F-G) Correlation between total and active PAI-1 and body weight. (H-I) PG was measured in 1:3-diluted normal, pooled plasma triggered with 1 pM TF and 0.31  $\mu$ g/mL rtPA in the presence of various concentrations of (H) total mouse and (I) conformationally-active human PAI-1. Bars indicate medians. Each dot represents a separate mouse. NS, not significant.

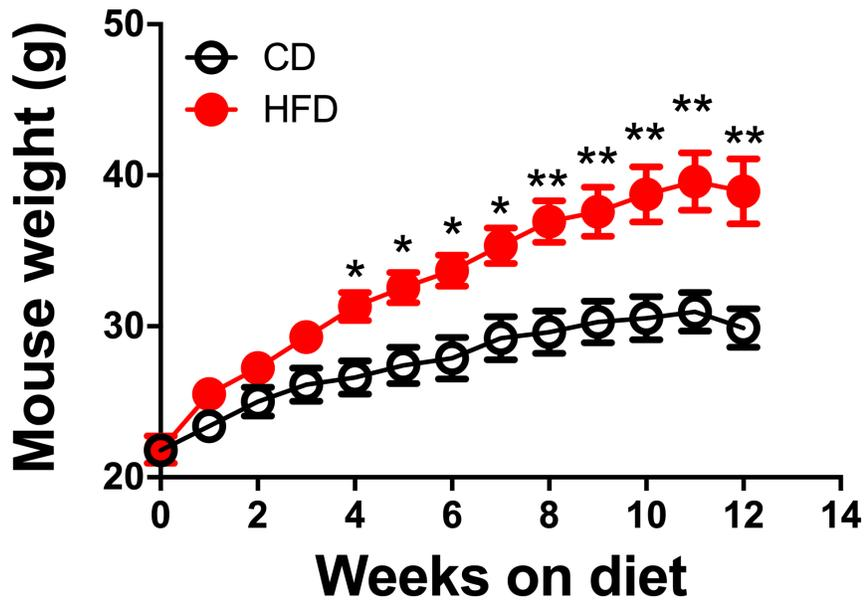
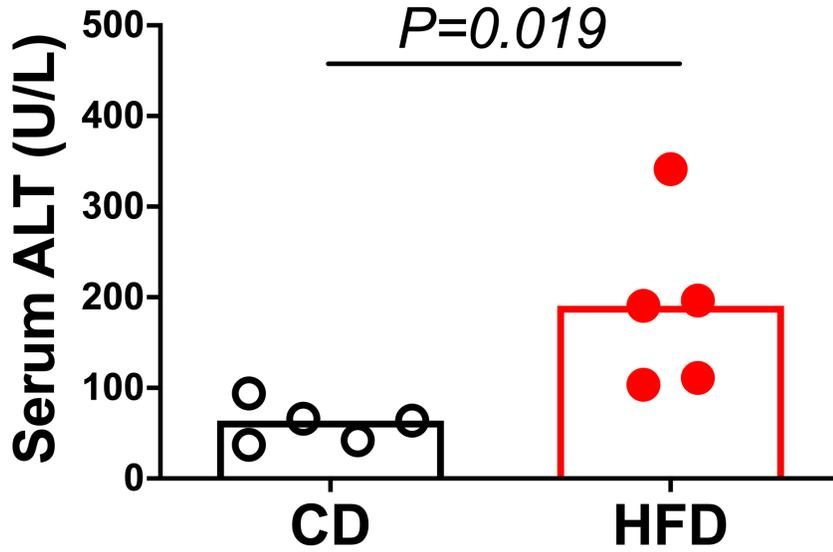
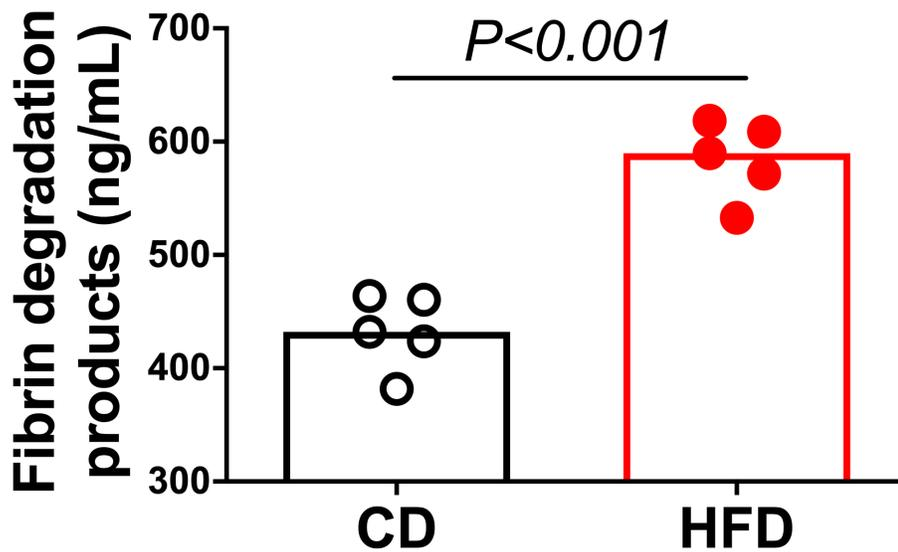
**Figure 5. Mass spectrometry detects altered concentrations of both coagulation and fibrinolytic proteins in plasma.** (A) Heat map with Ward clustering of protein relative abundances (Z-scored). (B) Partial least squares discriminant analysis data reduction based on relative abundances of plasma proteins from CD- (black circles) and HFD- (red circles) fed mice. (C) Enrichment of functional pathways in HFD-fed mice by KEGG analysis. (D-E) Relative C-1-inhibitor and TAFI levels in CD and HFD-fed mice determined by mass spectrometry. Intensity measurements are area under the curve for all peptides originating from the listed protein. (F) TAFI concentrations determined by ELISA. Bars indicate medians. Each dot represents a separate mouse.

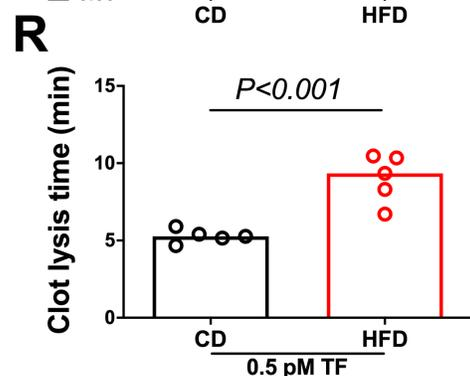
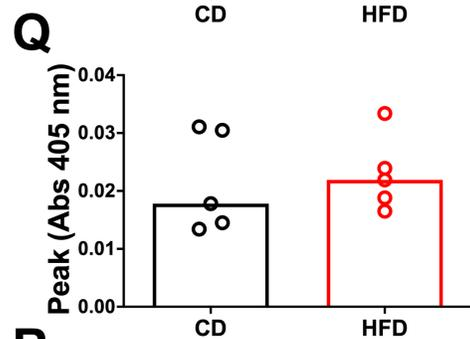
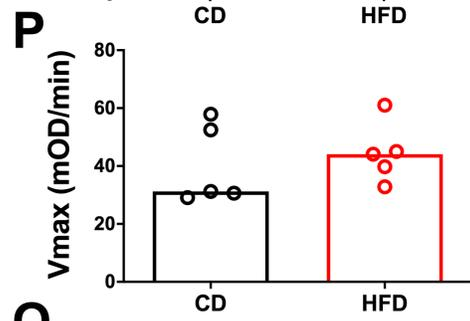
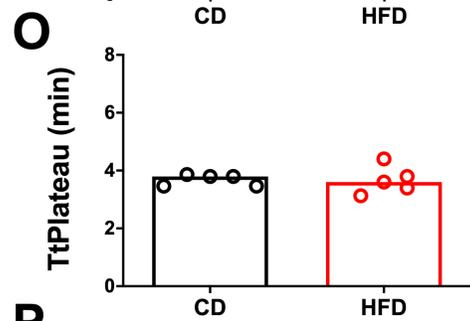
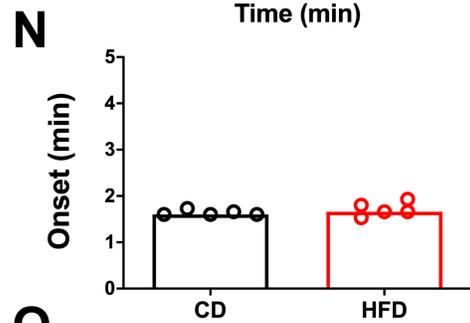
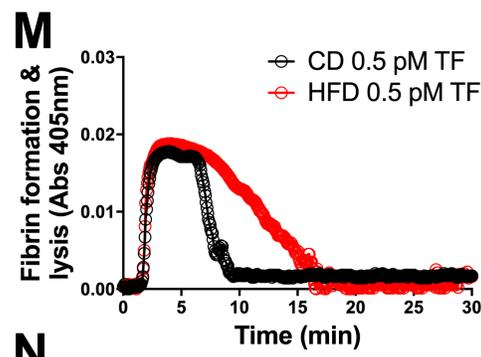
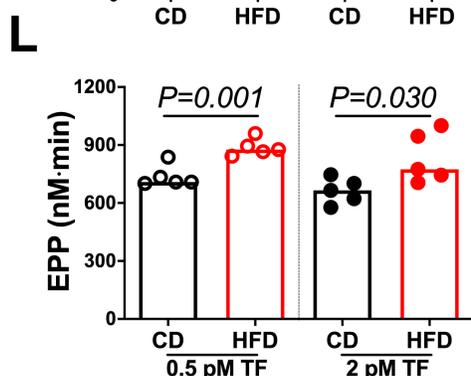
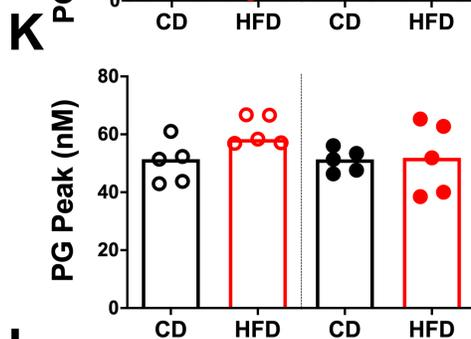
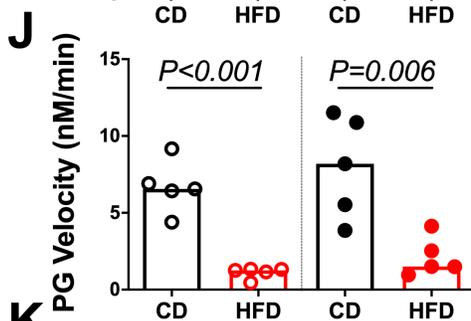
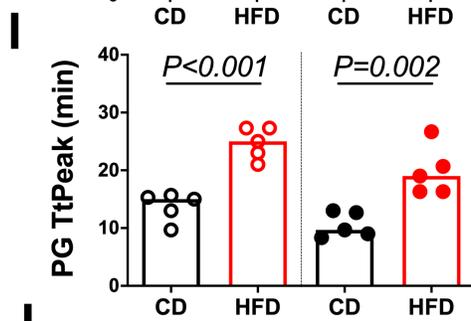
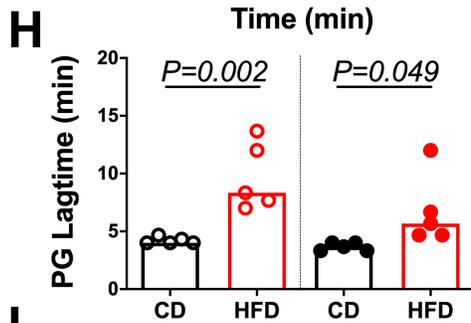
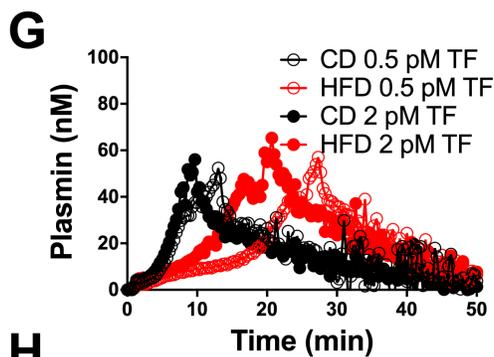
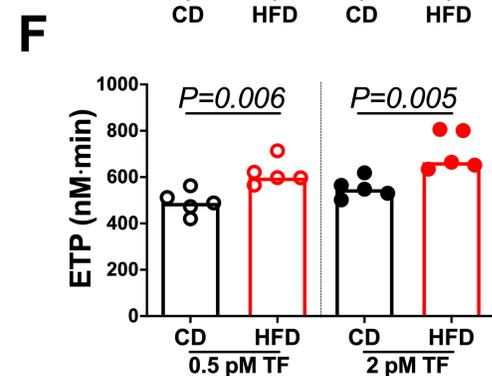
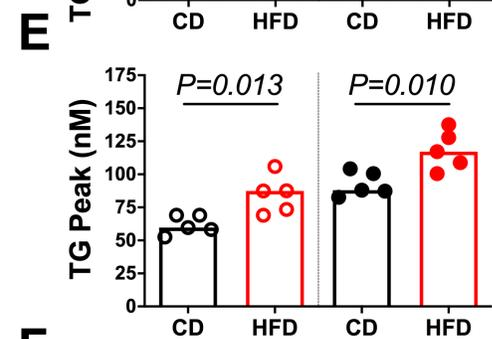
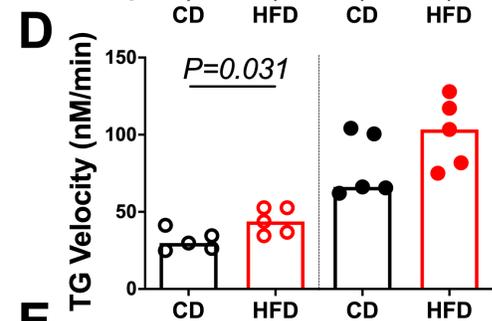
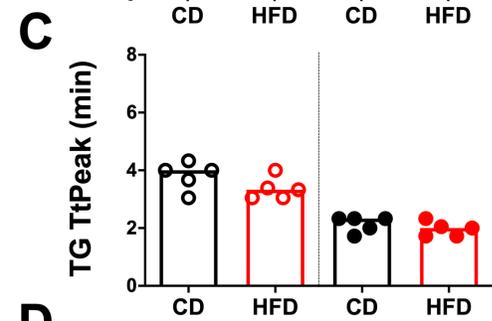
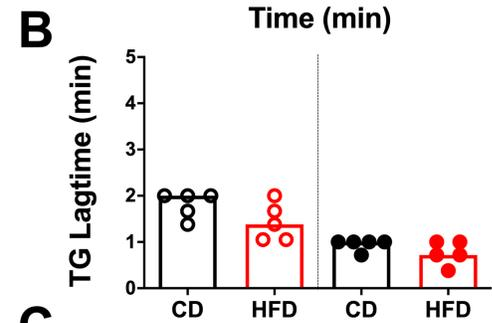
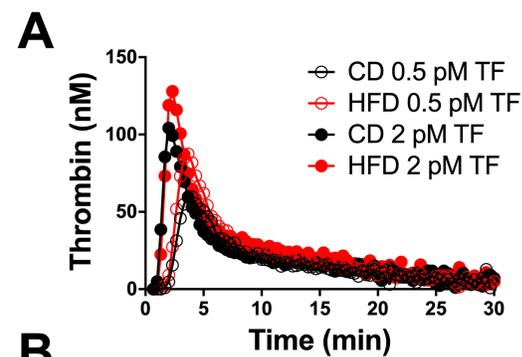
**Figure 6. Elevated thrombomodulin contributes to delayed PG via TAFI activation.** (A-B) PG was measured in the presence of increasing concentrations of exogenous (A) human C-1 inhibitor and (B) human TAFI. (C-D) Plasma from CD- and HFD-fed mice were separated by SDS-PAGE and immunoblotted with anti-thrombomodulin antibody. The major band indicated with an arrow in panel C was quantified in panel D. Each lane and dot represent a separate mouse in C and D, respectively. (E) TG, (F) PG, and (G) turbidity were measured in the presence of increasing concentrations of recombinant mouse thrombomodulin (rmTM, 0.31-10 nM) or potato tuber carboxypeptidase inhibitor (PTCI, 50  $\mu$ g/mL). (H) PG was measured in normal mouse plasma in the absence and presence of PTCI and anti-mouse thrombomodulin antibody (MTM-1701) or control IgG. (I-J) PG in plasma from CD- and HFD-fed mice in the absence and presence of MTM-1701 or PTCI. In this experiment, plasmas were from mice fed CD (13% kcal fat) or HFD (60% kcal fat) for 16 weeks. (K-O) PG parameters for CD- and HFD-fed mice in the absence or presence of MTM-1701 and PTCI. All experiments were performed in 1:3 diluted plasma, triggered with 0.5 pM TF and 0.31  $\mu$ g/mL rtPA (for PG and turbidity

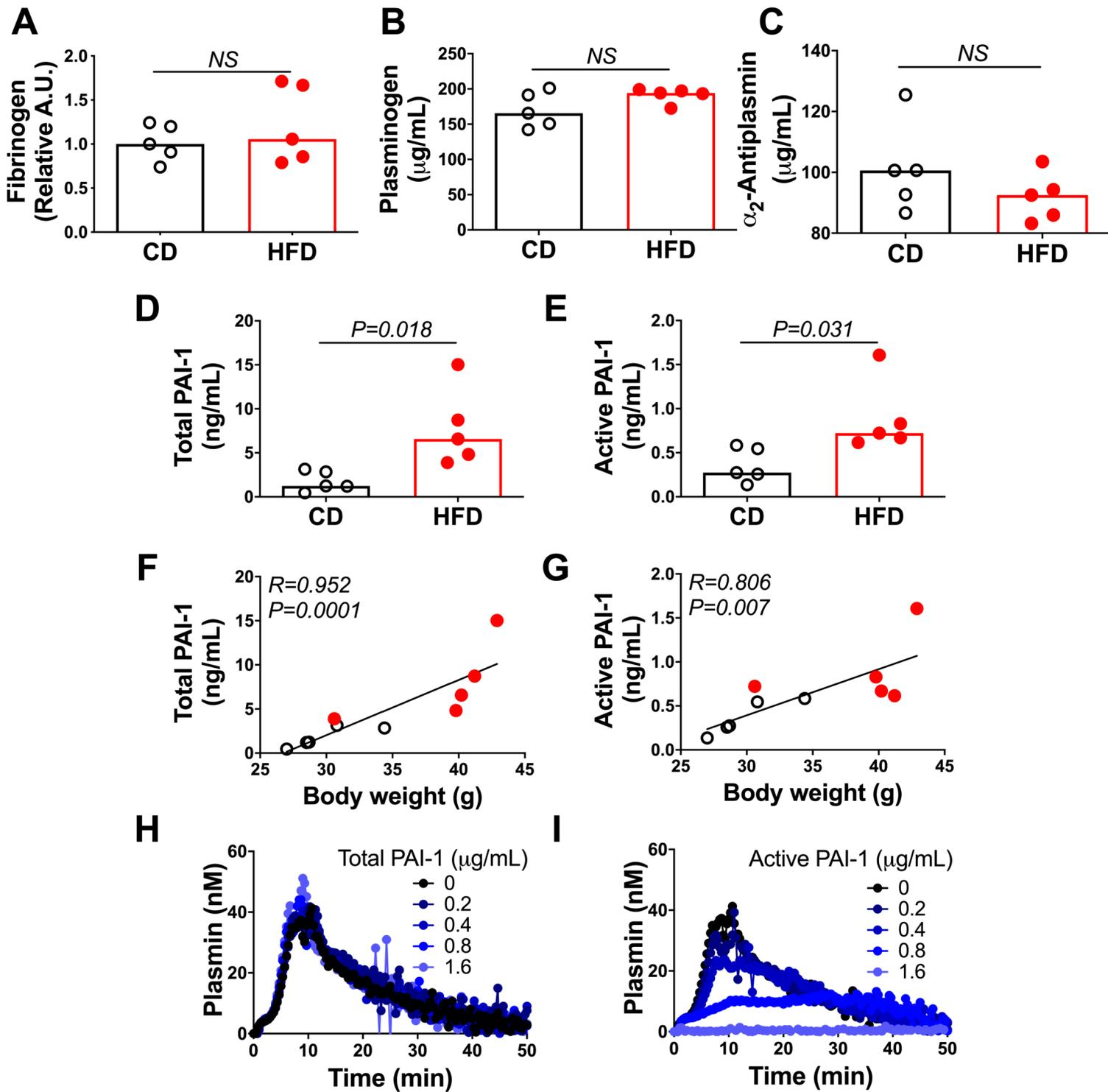
assays). Each dot represents a separate mouse. Bars indicate the medians. Statistical comparisons were performed by ANOVA with Dunnett's post-hoc testing, using CD or HFD as the index condition.  $P < 0.05$ ,  $**P < 0.01$ ,  $***P < 0.001$ , and  $****P < 0.0001$

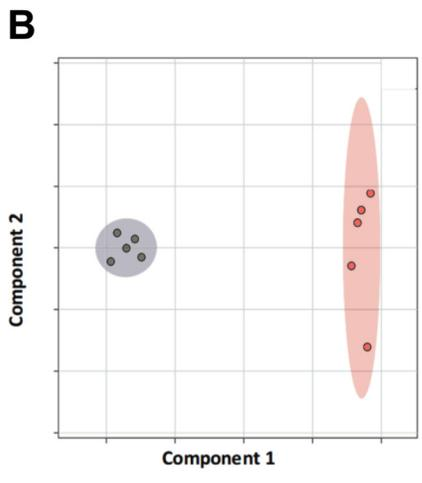
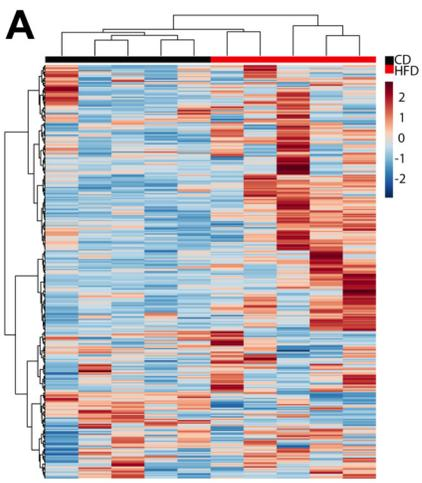
**Figure 7. TG/PG ratios reveal a prothrombotic phenotype in HFD-fed mice.** Representative curves of TG, PG, and turbidity for (A) CD-fed mice and (B) HFD-fed mice. TG/PG ratios were calculated by dividing each TG parameter by the corresponding PG parameter. Panels show TG/PG ratios for (C) lagtime, (D) TtPeak, (E) velocity, (F) peak, and (G) ETP/EPP. Bars indicate medians. Each dot represents a separate mouse.



**A****B****C**







**C**

KEGG Pathways			
Term Description	Observed Gene Count	Background Gene Count	False Discovery Rate
Complement and coagulation cascades	11	88	6.99x10 <sup>-5</sup>
Cholesterol metabolism	7	48	5.47x10 <sup>-5</sup>
PPAR signaling pathway	5	85	0.00061
Staphylococcus aureus infection	4	50	0.00111
Vitamin digestion and absorption	3	24	0.0024
Prion diseases	3	34	0.0051
Systemic lupus erythematosus	4	92	0.0056
Proteasome	3	45	0.0083
Lysosome	4	123	0.0125
Pertussis	3	74	0.0262

